Catalyst Synthesis of Silicon-Based Zn_2SiO_4−SiO_x Heterostructure Nanowires

H. Q. Wang, G. Z. Wang, L. C. Jia, C. J. Tang, and G. H. Li*

Key Laboratory of Materials Physics, Anhui Key Laboratory of Nanomaterials and Nanotechnology, Institute of Solid State Physics, Chinese Academy of Sciences, Hefei 230031, People's Republic of China

Received: June 20, 2007; In Final Form: July 30, 2007

In this paper, a simple catalyst synthesis strategy for the preparation of Si-based heterostructure nanowires has been reported. The heterostructure nanowires with 800 nm in length and 20 nm in diameter are composed of Zn_2SiO_4 and SiO_x nanowires in which the upper part is Zn_2SiO_4 nanowires and the lower part rooted to the Si substrate is SiO_x nanowires. Zn droplets catalyze the growth of SiO_x nanowires first, followed by each SiO_x nanowire splitting to several sub-branches of SiO_x nanowires, and Zn_2SiO_4 nanowires are formed at the end of the growth. It was found that the Si-based heterostructure nanowires form only at the relative low temperature. A dichromatic emission resulted respectively from SiO_x and Zn_2SiO_4 further proves the heterostructure. A possible growth mechanism was proposed to better understand the formation of the silicon-based heterostructure.

1. Introduction

Silicon (Si) is the basis for the majority of integrated electronic devices. It has been realized that nanostructruring of bulk semiconductors is an alternative approach to create artificial materials exhibiting specific properties. Si-based nanostructures have thus attracted much attention in recent years for their potential applications in one-dimensional quantum transistors, light-emitting diodes, and photonic crystals.[1,2] One-dimensional nanostructures are of both fundamental and technological interests and offer the opportunities to investigate electrical, optical, and thermal transport properties in size-confined systems in which the heterostructure is critical for the realization of nanoelectronic devices.[3−5] Different methods have been reported to synthesize the nanowire heterostructure, such as metal−organic vapor phase-eptiaxy method,[6,7] catalyst solution-liquid−solid synthesis,[8] hydrothermal method,[9] pulsed electrodeposition method in anodic alumina membranes,[10] and chemical vapor deposition (CVD) method.[11−14] The heterostructures have been shown to possess a variety of interesting and technologically relevant properties.[15−18] However, to date only a limited number of papers have been published on the growth of the Si-based heterostructures.[19] Therefore, it is essential to explore the strategy of combining the high-performance heterostructure nanowires with the Si technology.

Different metal catalysts, such as Sn, Ga, etc., have been used to guide the growth of Si-based SiO_2 nanowires by a CVD method.[20−23] Moreover, if the catalyst takes part in not only guiding the Si-based SiO_2 nanowire growth but also reacting with SiO_2 nanowire in a controlled experimental condition, a Si-based heterostructure could be produced. From the binary phase diagram, we know that Zn and Si can form a low melting point alloy at about 690 °C, therefore Zn can catalyze the growth of SiO_2 nanowire. Because the atomic sizes of Si (0.117 nm) and Zn (0.133 nm) and the electronegativities of Si (1.9) and Zn (1.65) are both comparable,[24] once Zn is oxidized to ZnO, it can easily diffuse into the SiO_2 nanowire lattice and form a Zn_2SiO_4 phase,[25] which is a promising functional material with a wide range of applications in phosphor host and catalyst.[26,27]

Herein, we present a catalyst synthesis method for the preparation of Si-based Zn_2SiO_4−SiO_x heterostructure nanowires. We demonstrated that Zn droplets could catalyze the growth of the SiO_x nanowires at the initial stage and finally react with SiO_x and form Zn_2SiO_4, leading to the formation of the Si-based heterostructure nanowire. It is expected that the heterostructure could be a remarkable example for synthesizing other Si-based heterostructures.

2. Experimental Section

2.1. Synthesis. In our experiments, Zn powders (99.999%) were used as a source material. Pure nitrogen (99.999% purity with O_2 and H_2O contents less than 4 and 3.5 molar ppm, respectively) was used as the carrier gas. Silicon (111) wafer (5×8 mm^2) was ultrasonically cleaned alternately in acetone and distilled water for 30 min before use. In a typical preparation, a ceramic boat filled with 1 g of Zn powders was placed at the center of an alumina tube, which was heated by a tube furnace. A silicon wafer substrate was placed in the middle part of an alumina boat situated at the downstream end of the alumina tube. Before heating, the pure nitrogen flowed through the furnace for about 20 min to clean impurity gas absorbed on the Si wafer, alumina boat, and the wall of the furnace. Then, the furnace was heated to 900 °C at a rate of 10 °C/min under a pressure of about 200 Torr, and the temperature of the alumina boat is at about 750 °C. The carrier gas was kept flowing through the tube during the experiment at a rate of 20 standard cubic centimeters per minute. After heating for a different time, the furnace was cooled down to room-temperature naturally. The temperatures at any point between the tube center and the tube's downstream end were monitored in situ by a sheathed thermocouple, allowing us to readily choose a proper temperature for the nanowires growth.

2.2. Characterization. The as-prepared products were characterized and analyzed by a field emission scanning electron microscope (FESEM, Sirion 200), high-resolution transmission electron microscope (HRTEM, JEOL 2010), energy dispersive X-ray spectroscope (EDS), and X-ray photoelectron spectroscopy (XPS, VGESCALAB MKII). A He−Cd laser system with

* Corresponding author. E-mail: ghli@issp.ac.cn.

10.1021/jp074783n CCC: $37.00
Published on Web 09/12/2007

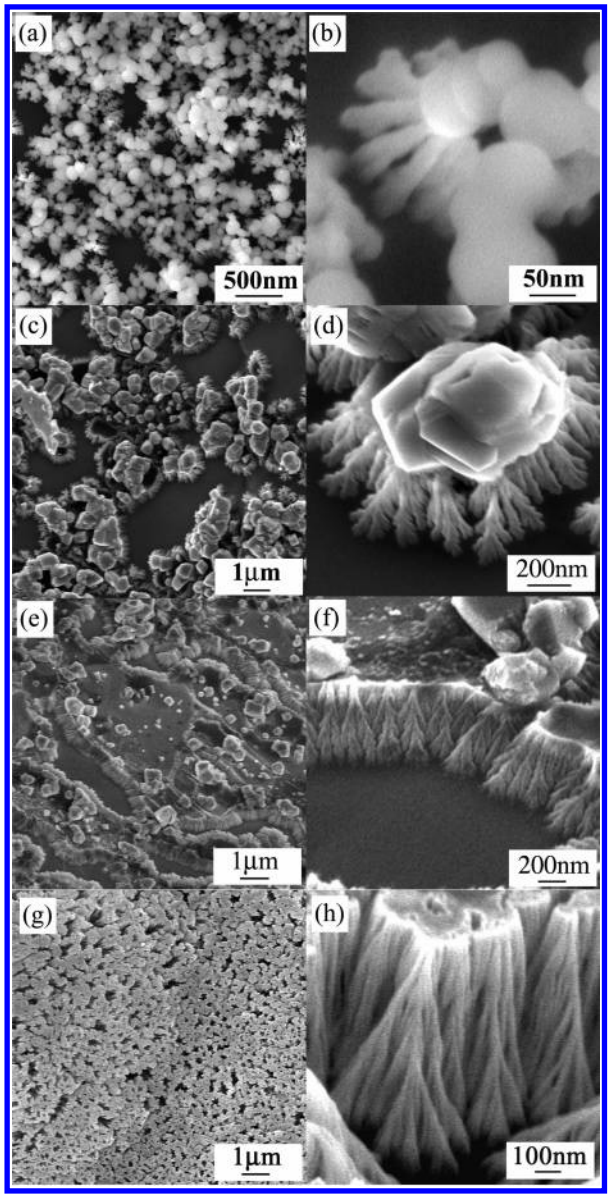

Figure 1. SEM image of $Zn_2SiO_4-SiO_x$ heterostructure nanowires grown at a time of (a,b) 45 min, (c,d) 60 min, (e,f) 90 min, and (g,h) 120 min.

the excitation wavelength of 325 nm was used to investigate the photoluminescence properties of the final products. As for the preparation of the TEM sample, the products were scraped off the silicon wafer and sonicated for several minutes in ethanol, then several drops of the solution were dripped on the carbon-coated copper grids.

3. Results and Discussion

3.1. Growth of the Si-Based Heterostructure Nanowires. Figure 1 shows the morphologies of products taken out from the furnace at different growth times at 750 °C. When heated for only 45 min, a large number of spheroid-nanowire structures with an average diameter of about 50 nm formed evenly on the surface of the silicon wafer (see Figure 1a). The high-magnification image shown in Figure 1b clearly indicates that each spheroid is attached with many nanowires with a length of about 100 nm that grow out from the lower surface of the spheroid. This is a typical image of vapor liquid solid (VLS) growth mechanism. This result demonstrates that each spheroid can simultaneously catalyze the growth of many nanowires, which is similar to the report in the literature,[20−23] and the only difference is the size of the catalyst; in present study, the size of the catalyst is only about 50 nm, while in the previous report it is several micrometers. It is noticeable that there is a bifurcation phenomenon of the nanowires in which each nanowire attached to the spheroid split into two branches, as shown in Figure 1b.

When the heating time increased to 60 min, two obvious changes are observed: (1) the shape of the catalyst on the nanowires transforms from spheroid to a relative regular shape, as shown in Figure 1c,d; (2) the length of the nanowires increases from 100 to about 200 nm, and the number of the nanowire bifurcation increases obviously in which many branches and sub-branches can be clearly seen. Only two branches in each nanowire can be observed for the product heat treated for 45 min, indicating a continuous growth of the nanowires.

As the heating time is prolonged to 90 min, the regular shape particles on the top of the nanowires of 60 min heating transforms to an inconspicuous thin layer covered on the well-aligned nanowires, which is shown in Figure 1e,f. In this heating time, the length of the nanowires increased to about 500 nm, and the bifurcation phenomenon continued. From the high magnification image shown in Figure 1e, one can see that there are still some regular shaped particles scattered on a large area surface of the nanowires, which might due to the continuous supply of Zn from the raw materials.

After heating for 120 min, highly aligned and closely packed stump-shaped nanowire-bundles are formed, as shown in Figure 1g,h. These bundles are almost perpendicular to the surface of the Si substrate and terminate at their top with a smooth surface, as demonstrated in Figure 1g. Several bundles are interconnected with each other and form a group, and each bundle is composed of nanowires with a uniform diameter of about 20 nm (see Figure 1h). It is worth noting that the split begins from the topside until the Si substrate in which each nanowire has several branches, and each branch has sub-branches with nearly the same diameter as the parent one. One also can clearly see that the nanowires root firmly with the silicon wafer indicating the nanowires grow from the silicon wafer. The energy-despersive spectrometry (EDS) analyses indicate that the upper part of the nanowire is composed of Zn, Si, and O elements, while the lower part is composed of only Si and O elements.

3.2. Characterization of the Si-Based Heterostructure Nanowires. Figure 2a shows a low-magnification TEM image of the heterostructure nanowire bundles. It can be observed that the lower part is intercrossed nanowires resulting from the bifurcation of the nanowires, which is in agreement with the SEM observations. The bifurcation phenomenon also can be observed in Figure 2b in which the dark area marked A is connected with three light areas marked B. The different contrasts between A and B indicate different crystallizations. The corresponding selected area electron diffraction (SAED) patterns shown in Figure 2c,d indicate that the dark area is a polycrystalline while the light area is an amorphous structure. This result can be further proved by HRTEM observations of the interface zone of the heterostructure nanowires, as shown in Figure 2e, which is the square area in Figure 2b. One can see that the left area of the white line (corresponding to the top part of square area in Figure 2b) is crystalline, while the right area (corresponding to the lower part of the square area in Figure 2b) is amorphous. The clear lattice fringe of the dark area in Figure 2f shows that the distances of the adjoined fringes are about 0.28 and 0.40 nm, corresponding respectively to the $(11\bar{3})$ and (300) planar distance of Zn_2SiO_4. The energy-dispersive

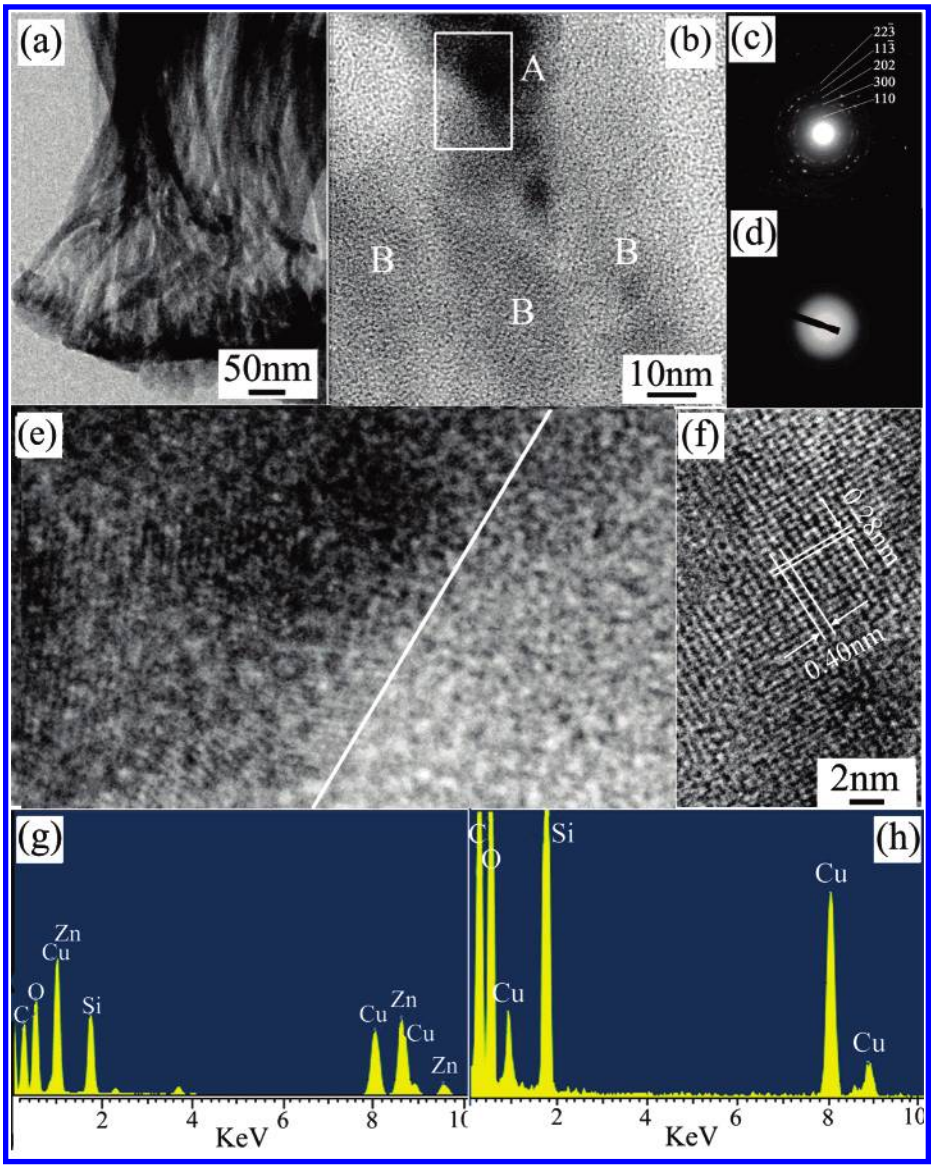

Figure 2. TEM images (a) $Zn_2SiO_4-SiO_x$ heterostructure nanowires bundles and (b) a $Zn_2SiO_4-SiO_x$ heterostructure nanowire, (c,g) the EDS and SAED patterns for Zn_2SiO_4 nanowires, respectively, (d,h) the EDS and SAED patterns for SiO_x nanowires, respectively, HRTEM image of (e) the interface zone in the square area in (b), and (f) lattice infringe image of the Zn_2SiO_4 nanowire.

X-ray analyses shown in Figure 2c,e clearly indicate the presence of Zn, Si, and O atoms in part A and Si and O in part B. The atomic ration of Si to O in part B is about 1.14, indicating the oxygen deficiency. These results proved that the nanowire bundle is a heterostructure in which the upper part is Zn_2SiO_4 and the lower part is SiO_x ($x < 2$).

The heterostructure of the nanowires was further confirmed by XPS analyses. Figure 3 shows the XPS results of the binding energy of Zn 2p3/2, Si 2p3/2 and O 1s of the final product. All peak positions were corrected by the C 1s peak at 284.6 eV. The Zn (2p3/2) peak is located at 1023.2 eV, and this slightly high-binding energy (usually situated below 1023 eV) is ascribed to the ternary compound.[28−30] The binding energies of O 1s at 532.9 and 531.5 eV are respectively attributed to Si−O bonds in SiO_4^{2-} and SiO_x.[31,32] An obvious band tail extending to the lower-binding energy side of Si 2p3/2 can be seen, indicating the coexistence of two different states of Si bonds, in which one is at 101.4 and the other at 102.9 eV through fitting. The peak at 101.4 eV is attributed to Si−O bonds in the SiO_x ($x < 2$) component, while that at 102.9 eV is attributed to the Si−O bonds within the SiO_4^{2-}.[33,34]

It is well known that Zn_2SiO_4 is a green luminescent material,[35,36] and SiO_2 has been a bright blue emitter.[37,38] Figure 4 shows the PL spectrum of the $Zn_2SiO_4-SiO_x$ heterostructure nanowires. A blue emission centered at about 404 nm attributed to SiO_2 and a green emission situated at about 521 nm related to Zn_2SiO_4 can be clearly seen. The relative stronger emission strength from Zn_2SiO_4 compared with that reported in the literature[25] maybe due to the fact that the upper part of the heterostructure is covered with Zn_2SiO_4, while the lower part is SiO_x. These results further confirmed the coexistence of Zn_2SiO_4 and SiO_x components in the heterostructure nanowires.

To further investigate if Zn exists as a catalyst at the initial stage of the nanowires, we analyze the XPS profiles of the products heated for 45 min. The results clearly show that there is pure Zn at the initial growth stage of the nanowire bundles, as shown in Figure 5, in which an obvious difference can be seen as compared with that shown in Figure 3. The Zn 2p peak shown in Figure 5a is at 1021.8 eV and is 1.5 eV lower than that shown in Figure 3a, indicating the existence of another bonding state of Zn. By fitting, two peaks are obtained: one is centered at 1021.3 eV and the other at 1022.0 eV, indicating

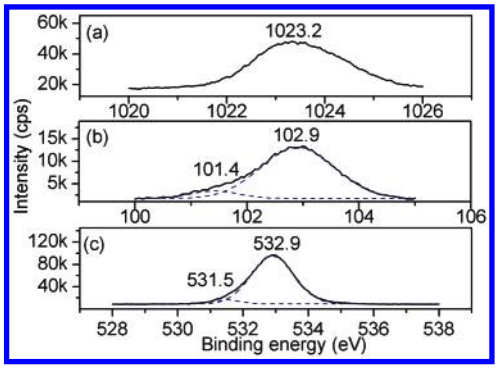

Figure 3. XPS profiles of (a) Zn 2p3/2, (b) Si 2p3/2, and (c) O 1s for $Zn_2SiO_4-SiO_x$ heterostructure nanowires synthesized at 900 °C for 120 min.

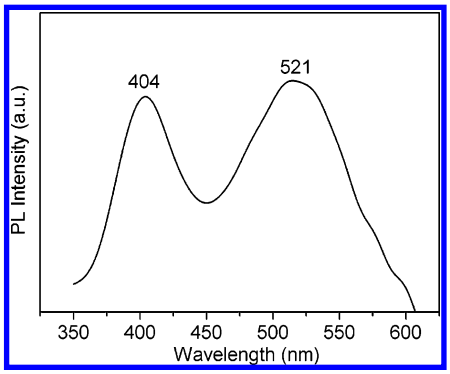

Figure 4. PL spectrum of $Zn_2SiO_4-SiO_x$ heterostructure nanowires.

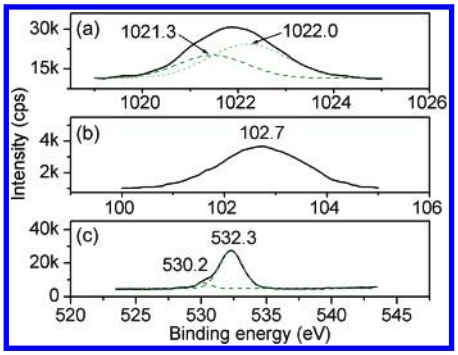

Figure 5. XPS profiles of (a) Zn 2p3/2, (b) Si 2p3/2, and (c) O 1s for $Zn_2SiO_4-SiO_x$ heterostructure nanowires synthesized at 900 °C for 45 min.

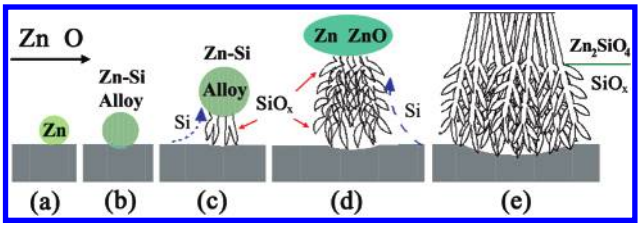

Figure 6. Schematic illustration of the growth mechanism of $Zn_2SiO_4-SiO_x$ heterostructure nanowires. (a) Zn clusters deposit onto the silicon surface and form a small droplet; (b) Zn droplet etches silicon wafer and forms spheroidlike Zn−Si alloy; (c) the growth of SiO_x nanowires from the spheroid; (d) continued growth up of SiO_x-nanowires; and (e) formation of $Zn_2SiO_4-SiO_x$ heterostructure nanowires.

the coexistence of Zn^0 and ZnO, which is in agreement with the previous report.[39] The perfect Gassian symmetry of the Si 2p3/2 peak centered at 102.7 eV indicates that there is only one bonding state for Si (see Figure 5b) corresponding to SiO.[40] The asymmetry feature of O 1s can be clearly seen in Figure 5c, and by fitting a small peak centered at 530.2 eV is obtained, which corresponds to O−Zn bond,[41] while the peak centered at 532.3 eV corresponds to Si−O bond in SiO.[40] The qualitative analyses indicate that the atomic ratio of Zn^0 to Zn^{+2} is about 1.8:1, further indicating the existence of Zn^0. The expansion of the band tail of Zn Auger peak to 991 eV provides more evidence of the existence of Zn^0.[42] These results proved that the Zn clusters first formed on the surface of Si substrate, and some of them transformed to ZnO. The transformation from Zn to ZnO is considered due partly to the remaining O_2 in the carrying gas and partly to the oxidation of the small Zn particles in the cooling process.

3.3. Formation Mechanism of the Si-Based Heterostructure Nanowires. The relative low temperature in the growth area is a very important factor in controlling the formation of the heterostructure nanowires. If the temperature is too lowe, such as 400 °C, it is impossible to form the Zn−Si alloy and no SiO_x nanowire is formed except Zn/ZnO nanoropes, and if the temperature is too highe, such as 850 °C, the Zn−Si alloy will oxide to Zn_2SiO_4 directly, forming only rowlike Si-based Zn_2SiO_4 nanowires. Additionally, it was found that the carrying gas, including the flow rate and content of oxygen, also play an important role in the formation of the $Zn_2SiO_4-SiO_x$ heterostructure nanowires. If the oxygen content is too highe, the Zn droplets will be oxidized immediately, and no Zn_2SiO_4 nanowires are formed; if there is no oxygen in the carrier gas, Si nanowires will be catalyzed by the Zn droplets.

On the basis of the above results, a growth mechanism is proposed as schematically illustrated in Figure 6. First, the Zn powders are vaporized into small Zn clusters at the temperature of about 900 °C, then the clusters downstream transfer to the alumina tube by the carrier gas and deposit onto the surface of Si substrate at the temperature of about 750 °C. The accumulated Zn clusters transform to a Zn liquid droplet, and the droplet reacts with silicon and forms a supersaturated low melting point Zn−Si alloy with some resolved oxygen. As the Si in Zn−Si low melting alloy reaches the solubility, Si begins to separate out from the Zn−Si solid solution and is oxidized to SiO_2 nanoparticles. Because the bond energy of Si−O bond (185 kJ/mol) is about two times higher than that of the Zn−O bond (92 kJ/mol), Si in the Zn−Si solid solution will preferentially react with O to form stable SiO_x. The direct formation of Zn_2SiO_4 phase from Zn, Si, and O needs a higher temperature as described above and reported in literature,[43]and the low temperature of 750 °C favors the formation of SiO_2 instead of Zn_2SiO_4 at the initial growth stage. The SiO_x formed simultaneously at the above two processes will accumulate into SiO_x nanoparticles on the lower surface of the Zn spheroid. These particles act as the nucleation sites and initiate the growth of SiO_x nanowire, and the Zn(Si) spheroid is then pushed away from the Si wafer by the growing nanowires, which will lead to the decrease of Si content in the Zn spheroid. During the continuous growth of the SiO_x nanowires, the newly formed SiO_x clusters adsorbed on the side of the nanowires controlled by side surface mass diffusion as reported by Hao et al.[44] will react as new nucleation centers guiding the growth of branch nanowires and leading to a bifurcation growth phenomenon. The decreased Si could simultaneously be supplied by the surface diffusion from the Si wafer upward to the Zn spheroid along the growth direction of the nanowire.[45] However, the supplement of Si from the Si wafer is confined in a limited distance because of the relative low reaction temperature, and finally when the nanowires grow to a critical length the Si in the Zn spheroid will be consumed and the SiO_x nanowires stop growing. Subsequently, the Zn spheroid is oxidized slowly for the absence of competi-

tion between Si−O and Zn−O bonding. Because the Si atom has nearly the same diameter as the Zn atom, it is easy for ZnO to diffuse into the SiO_x nanowire and form Zn_2SiO_4 phase as proposed by Wang et al.[21] With the continuous supply of Zn from the vapor, the length of the Zn_2SiO_4 nanowire increases until the Zn source was completely consumed. Finally, the Zn_2SiO_4 nanowires grow on the top of the SiO_x nanowire and the $Zn_2SiO_4-SiO_x$ heterostructure nanowires are formed.

4. Conclusions

Well oriented and closely packed Si-based $Zn_2SiO_4-SiO_x$ ($x < 2$) heterostructure nanowires have been prepared via a catalyst synthesis approach. The heterostructure nanowires are composed of Zn_2SiO_4 nanowires at the upper part and SiO_x nanowires at the lower part, and the SiO_x nanowire splits to several subbranches of SiO_x nanowire in the Si substrate direction. The XPS analysis proved the formation of Zn_2SiO_4 and SiO_x and the existence of the Zn catalyst at the initial stage. The dichromatic PL emission from SiO_x and Zn_2SiO_4 further proved the heterostructure of the nanowires. It was found that the relative low growth temperature plays an important role in the formation of the heterostructure nanowires. The formation of the heterostructure nanowires undergoes two processes: Zn droplets catalyze the growth of the SiO_x nanowires by a VLS mechanism, and then ZnO diffuses into the SiO_x forming Zn_2SiO_4 nanowires at the end of the growth. The Si-based $Zn_2SiO_4-SiO_x$ heterostructure nanowires are expected to find potential applications in optoelectronic devices.

Acknowledgment. This work was supported by the National Major Project of Fundamental Research for Nanomaterials and Nanostructures (2005CB623603).

Supporting Information Available: The XRD pattern of product synthesized at 400 °C, SEM image of product synthesized at 850 °C, XPS analyzed results and Auger spectrum of the Zn^0 heated for 45 min at 750 °C. This material is available free of charge via the Internet at http://pubs.acs.org.

References and Notes

(1) Alivisatos, A. P. *Science* **1996**, *271*, 933.
(2) Park, J.-H.; Derfus, A. M.; Segal, E.; Vecchio, K. S.; Bhatia, S. N.; Sailor, M. J. *J. Am. Chem. Soc.* **2006**, *128*, 7938.
(3) Patolsky, F.; Gill, R.; Weizmann, Y.; Mokari, T.; Banin, U.; Willner, I. *J. Am. Chem. Soc.* **2003**, *125*, 13918.
(4) Yu, D. P.; Hang, Q. L.; Ding, Y.; Zhang, H. Z.; Bai, Z. G.; Wang, J. J.; Zou, Y. H.; Qian, W.; Xiong, G. C. and Feng, S. Q. *Appl. Phys. Lett.* **1998**, *73*, 3076.
(5) Yang, C.; Zhong, Z. H.; Lieber, C. M. *Science* **2005**, *310*, 1304.
(6) Verheijen, M. A.; Immink, G.; Smet, T.; Borgström, M. T.; Bakkers, E. P. A. M. *J. Am. Chem. Soc.* **2006**, *128*, 1353.
(7) Park, W. I.; Yoo, J.; Kim, D. W.; Yi, G. C.; Kim, M. *J. Phys. Chem. B* **2006**, *110*, 1516.
(8) Ouyang, L.; Maher, K. N.; Yu, C. L.; McCarty, J.; Park, H. K. *J. Am. Chem. Soc.* **2007**, *129*, 133.
(9) Du, J. M.; Fu, L.; Liu, Z. M.; Han, B. X.; Li, Z. H.; Liu, Y. Q.; Sun, Z. Y.; Zhu, D. B. *J. Phys. Chem. B* **2005**, *109*, 12772.
(10) Xue, F. H.; Fei, G. T.; Wu, B.; Cui, P.; Zhang, L. D. *J. Am. Chem. Soc.* **2005**, *127*, 15348.
(11) Choi, H. J.; Shin, J. H.; Suh, K.; Seong, H. K.; Han, H. C.; Lee, J. C. *Nano Lett.* **2005**, *5*, 2432.
(12) Shen, G. Z.; Bando, Y.; Tang, C. C.; Golberg, D. *J. Phys. Chem. B* **2006**, *110*, 7199.
(13) Ha, B.; Kim, H. C.; Kang, S. G.; Kim, Y. H.; Lee, J. Y.; Park, C. Y.; Lee, C. J. *Chem. Mater.* **2005**, *17*, 5398.
(14) Jung, Y.; Ko, D. K.; Agarwal, R. *Nano Lett.* **2007**, *7*, 264.
(15) Hu, J. T.; Ouyang, M.; Yang, P. D.; Lieber, C. M. *Nature* **1999**, *399*, 48.
(16) Wang, Z. L.; Dai, Z. R.; Gao, R. P.; Bai, Z. G.; Gole, J. L. *Appl. Phys. Lett.* **2000**, *77*, 3349.
(17) Shen, G. Z.; Bando, Y.; Golberg, D. *J. Phys. Chem. B* **2006**, *110*, 23170.
(18) Schierhorn, M.; Lee, S. J.; Boettcher, S. W.; Stucky, G. D.; Moskovits, M. *Adv. Mater.* **2006**, *18*, 2829.
(19) Herman, M. A. *Cryst. Res. Technol.* **1999**, 34, 583.
(20) Pan, Z. W.; Dai, S.; Beach, D. B.; Lowndes, D. H. *Appl. Phys. Lett.* **2003**, *83*, 3159.
(21) Pan, Z. W.; Dai, Z. R.; Ma, C.; Wang, Z. L. *J. Am. Chem. Soc.* **2002**, *124*, 1817.
(22) Sun, S. H.; Meng, G. W.; Zhang M. G.; Hao, Y. F.; Zhang X. R.; Zhang L. D. *J. Phys. Chem. B* **2003**, *107*, 13029.
(23) Xiao, Z. D.; Zhang, L. D. Meng, G. W.; Tian X. K.; Zeng H. B.; Fang, M. *J. Phys. Chem. B* **2006**, *110*, 15724.
(24) An, X. H.; Meng, G. W.; Wei, Q.; Zhang, L. D. *Cryst. Growth Des.* **2006**, *6*, 1967.
(25) Wang, X. D.; Summers, C. J.; Wang, Z. L. *Adv. Mater.* **2004**, *16*, 1215.
(26) Bartohu, C.; Benoit, J.; Benalloul, P.; Morell, A. *J. Electrochem. Soc.* **1994**, *141*, 524.
(27) Breure, K.; Teles, J. H.; Demuth, D.; Hibst H.; Schäfer, A.; Brode, S.; Domgörgen, H. *Angew. Chem., Int. Ed.* **1999**, *38*, 1401.
(28) Nefedov, V. I. *J. Electron Spectrosc. Relat. Phenom.* **1982**, *25*, 29.
(29) Strohmeier, B. R.; Hercules, D. M. *J. Catal.* **1984**, *86*, 266.
(30) Dake, L. S.; Baer, D. R.; Zachara, J. M. *Surf. Interface Anal.* **1989**, *14*, 71.
(31) Wagner, C. D.; Zatko, D. A.; Raymond, R. H. *Anal. Chem.* **1980**, *52*, 1445.
(32) Cros, A.; Saoudi, R.; Hewett, C. A.; Lau, S. S.; Hollinger, G. *J. Appl. Phys.* **1990**, *67*, 1826.
(33) Nguyen, T. P.; Lefrant, S. *J. Phys. Condens. Matter* **1989**, *1*, 5197.
(34) Lorenz, P.; Finster, J.; Wendt, G.; Salyn, J. V.; Zumadilov, E. K.; Nefedov, V. I. *J. Electron Spectrosc. Relat. Phenom.* **1979**, *16*, 267.
(35) Wan, J. X.; Chen, X. Y.; Wang, Z. H.; Mu, L.; Qian, Y. T. *J. Cryst. Growth* **2005**, *280*, 239.
(36) Zhou, J.; Liu, J.; Wang, X. D.; Song, J. H.; Tummala, R.; Xu, N. S.; Wang Z. L. *Small* **2007**, *3*, 622.
(37) Yu, D. P.; Hang, Q. L.; Ding, Y.; Zhang, H. Z.; Bai, Z. G.; Wang, J. J.; Zou, Y. H.; Qian, W.; Xiong, G. C.; Feng S. Q. *Appl. Phys. Lett.* **1998**, *73*, 3076.
(38) Hao, Y. F.; Meng, G. W.; Ye, C. H.; Zhang, L. D. *Appl. Phys. Lett.* **2005**, *87*, 033106.
(39) Liu, B.; Zeng, H. C. *J. Am. Chem. Soc.* **2004**, *126*, 16744.
(40) Taylor, J. A.; Lancaster, G. M.; Ignatiev, A.; Rabalais, J. W. *J. Chem. Phys.* **1978**, *68*, 1776.
(41) Agostinelli, E.; Battistoni, C.; Fiorani, D.; Mattogno, G.; Nogues, M. *J. Phys. Chem. Solids* **1989**, *50*, 269.
(42) Kowalczyk, S. P.; Pollak, R. A.; McFeely, F. R.; Ley, L.; Shirley, D. A. *Phys. Rev. B* **1973**, *8*, 2387.
(43) Feng, X.; Yuan, X. L.; Sekiguchi, T.; Lin, W. Z.; Kang, J. Y. *J. Phys. Chem. B* **2005**, *109*, 15786.
(44) Hao, Y. F.; Meng, G. W.; Wang, Z. L.; Ye, C. H.; Zhang, L. D. *Nano Lett.* **2006**, *6*, 1650.
(45) Verheijen, M. A.; Immink, G.; Smet, T.; Borgström, M. T.; Bakkers, E. P. A. M. *J. Am. Chem. Soc.* **2006**, *128*, 1353.